

Activation mechanism of lead ion in the flotation of stibnite

Qinbo Cao^{a,b}, Xiumin Chen^{a,*}, Qicheng Feng^{a,b,*}, Shuming Wen^{a,b}

^a State Key Laboratory of Complex Nonferrous Metal Resources Clean Utilization, Kunming 650093, PR China

^b Faculty of Land Resources Engineering, Kunming University of Science and Technology, Kunming 650093, Yunnan, PR China



ARTICLE INFO

Keywords:

Stibnite
Flotation
Activation
Lead ion
Density functional theory

ABSTRACT

The flotation of stibnite with Pb^{2+} as an activator was examined with micro-flotation tests, inductively coupled plasma mass spectrometry (ICP-MS) experiments and density functional theory (DFT) calculations. It was found that at a pH of 6.5, the addition of $Pb(NO_3)_2$ notably improved the flotation efficiency of stibnite with butyl xanthate (BX). At a pH of 6.5, Pb^{2+} was the dominant species adsorbing at the stibnite surface. DFT calculations implied that Pb^{2+} could adsorb at five different sites on the stibnite surface. Furthermore, BX could adsorb onto the Pb sites at the Pb-activated surface and the Sb sites of the un-activated surface, while the adsorption of BX on the Pb-activated surface is more stable.

Partial density of states (PDOS) analysis revealed that the poor overlapping between the S 3p orbital of BX and the Sb 5s orbital accounts for the weak interaction between BX and the un-activated surface. For the Pb-activated surface, the Pb 6p orbital and the S 3p orbital of BX were efficiently overlapped with each other, resulting in a relatively stronger interaction between BX and the activated surface. The DFT simulation provides a deep insight into the role of Pb^{2+} during the activation flotation of stibnite.

1. Introduction

Antimony is an important component in the production of flame retardants, batteries and alloys (Anderson, 2012). In the United States, approximately 57% of antimony is consumed for the production of flame retardants (Butterman and Carlin, 2004). More than 100 antimony bearing-minerals have been found in nature (Anderson, 2012), while stibnite (Sb_2S_3) is one of the most common ores in deposits and is the predominant ore in industry (Lager and Forssberg, 1989).

Flotation is an efficient method to separate stibnite from other gangue minerals. Stibnite can be efficiently floated by xanthates in an acidic medium below pH 5 (Huang, 1987). At a pH above 5, stibnite does not respond well to xanthates. Due to the presence of alkaline gangues in most deposits, it is not economical to float stibnite in an acidic slurry. Instead, the flotation of stibnite is conducted at natural pH (about pH 6.5) using lead nitrate as an activator (Vijayakumar and Majumdar, 1972). This method has been successfully used in industry (Lager and Forssberg, 1989).

The application of $Pb(NO_3)_2$ in the activation of mineral flotation has attracted considerable interest. It has been well established that Pb^{2+} can promote the flotation of sphalerite and pyrite (Xia et al., 2015). In the flotation system of ilmenite, the use of $Pb(NO_3)_2$ enhances the adsorption of oleate at the ilmenite surface rather than at the quartz surface (Chen et al., 2017; Fan and Rowson, 2000). Li et al. proposed

that the Pb^{2+} could improve the floatability of rutile with salicyl hydroxamic acid (SHA) (Li et al., 2016), while the adsorption of SHA at the cassiterite surface can also be improved by the addition of Pb^{2+} (Feng et al., 2017a). In the above systems, the effect of Pb species on mineral flotation has been investigated in detail. However, less research has addressed the activation features of $Pb(NO_3)_2$ for the stibnite flotation.

An X-ray photoelectron spectroscopy (XPS) study indicated that a film of PbS formed at the stibnite surface after the stibnite was conditioned with a $Pb(NO_3)_2$ solution (Nefedov et al., 2010). It is generally believed that the activation effect of Pb^{2+} depends on the surface adsorption of Pb^{2+} at the stibnite surface. As expected, the substitution of the Pb atom for the Sb atom at the stibnite surface could also occur (Solozhenkin et al., 1991). However, aside from the XPS results, no further study was provided to reveal the adsorption or substitution behavior of Pb^{2+} at the stibnite surface.

First-principles calculation, based on density functional theory (DFT), has become an important research tool in flotation chemistry (Feng et al., 2017b, 2017c). This simulation method is reliable when assessing the chemical features of collectors (Zhao et al., 2013; Zhong et al., 2008) and the surface energetics of minerals (Hung et al., 2002; Wen et al., 2013; Zhu and Wu, 2004). More importantly, this method is widely used in the analysis of the chemical interaction between a collector and mineral surface (Chen et al., 2013; Liu et al., 2014; Rath

* Corresponding authors at: State Key Laboratory of Complex Nonferrous Metal Resources Clean Utilization, Kunming 650093, PR China (Q. Feng).
E-mail addresses: chenxiumin9@hotmail.com (X. Chen), fqckmust@163.com (Q. Feng).

et al., 2014; Zhu et al., 2016). Zhao et al. investigated the frontier orbital features of stibnite (Zhao et al., 2015), and the adsorption of $\text{Ca}(\text{OH})^-$ at the stibnite surface was further evaluated by the frontier orbital results. Solozhenkin found that a butyl xanthate molecule could bind to the Pb atom in a stibnite cluster model (Solozhenkin and Ibragimova, 2015).

The structure of the stibnite surface is complex, consisting of parallel ribbon-like $(\text{Sb}_4\text{S}_6)_n$ polymers (Zakaznova-Herzog et al., 2006). It is reasonable to expect that various sites existing at the stibnite surface allow for the adsorption of Pb^{2+} . The position of Pb on the stibnite surface, to some extent, determines the interactions that occur between the butyl xanthate (BX) and Pb atom. The adsorption site of Pb^{2+} on the stibnite surface and its influence on the xanthate adsorption have still not been fully investigated.

Until now, our knowledge regarding the activation flotation of stibnite with Pb^{2+} is not satisfactory. This paper aims to reveal the underlying activation-mechanism of Pb^{2+} in the flotation of stibnite. First, the effect of $\text{Pb}(\text{NO}_3)_2$ on the flotation of stibnite with BX was re-examined with micro-flotation tests. The concentrations of metal ions in the solution were measured to analyze the ion-substitution at the stibnite surface. Furthermore, the possible interaction models between BX, Pb^{2+} and the stibnite surface were generated with a DFT simulation. The adsorption properties of BX at the un-activated and Pb-activated surface were compared to assess the Pb atom effect at the mineral surface for the flotation of stibnite.

2. Materials and methods

2.1. Sample and reagents

Stibnite pebbles were provided from Yunnan Muli Antimony Industry Co., Ltd., China. The chemical analysis suggests that the stibnite sample contains 71.60% of Sb and 28.27% of S, and further the X-ray diffraction (XRD) pattern of stibnite sample indicates that the purity of stibnite was higher than 99% (Fig. 1). Sodium butyl xanthate (NaBX), lead nitrate, hydrochloric acid and sodium hydroxide were all AR grade and were purchased from Sinopharm Chemical Reagent Co., Ltd., China. Pine oil was obtained from Hunan Minzhu Flotation Reagents Co., Ltd., China. Deionized water (DI water) was used for the experimental study. All the tests were conducted at a pH of 6.5.

2.2. Micro-flotation test

A XFGCII flotation machine with a 100-mL flotation cell was employed for the micro-flotation study. This flotation machine was purchased from Jilin Province Ore Exploration Machinery Factory, China.

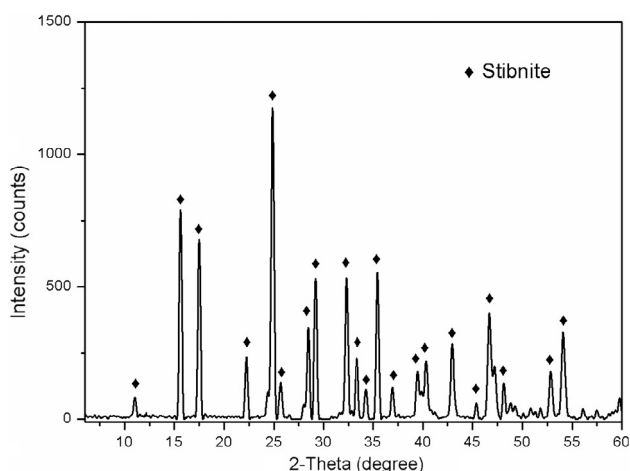


Fig. 1. XRD pattern of the pure stibnite sample.

Pure mineral (3.0 g, –100 mesh +150 mesh) was used in each test. The sample was first conditioned with a lead nitrate solution for 1 min, after which the collector was added into the solution, followed by further stirring for 1 min. The concentration of pine oil in the solution was 40 mg/L, and conditioning time for the frother was 1 min. The flotation time was controlled to 2 min, during which the air flow rate was 30 mL/min. The froth product and sink products were collected to calculate the recovery, and each test was repeated three times.

2.3. ICP-MS analysis

Inductively coupled plasma mass spectrometry (ICP-MS) analysis was conducted with a Penexion 350x. Stibnite powder (3 g, –100 mesh +150 mesh) was added into 100 mL of DI water, and the suspension was stirred for 30 min. A desired amount of lead nitrate was then added into the suspension, and after 3 min of conditioning, the suspension was centrifuged to obtain a clear liquid. The concentrations of Pb and Sb in the clear liquid were measured using the ICP-MS technique. The error of measurement was less than 10%.

2.4. Computational details

The DFT calculations were conducted using the program package Cambridge Sequential Total Energy Package (CASTEP) code (Segall et al., 2002). Generalized gradient approximation (GGA) in the scheme of Perdew-Burke-Ernzerhof functional was used to treat the exchange and correlation potentials (Perdew et al., 1996; Perdew and Zunger, 1981). Ultrasoft pseudo-potential was used to describe the interactions between the ionic core and valence electrons (Francis and Payne, 1990). The valence electron configurations for the elements are H $1s^1$, C $2s^2 2p^2$, O $2s^2 2p^4$, S $3s^2 3p^4$, Sb $5s^2 5p^3$ and Pb $5d^{10} 6s^2 6p^2$. The calculation of spin-polarization was performed during the simulation. The TS dispersion force correction method, developed by Tkatchenko and Scheffler, was used to describe the noncovalent forces (Tkatchenko and Scheffler, 2009). The energy convergence was set as 1×10^{-6} eV/atom. The Brillouin-zone integrations were performed using a $3 \times 3 \times 1$ k-point mesh and plane wave cutoff energy of 380.0 eV was used for the calculation. The parameters of k-points and cutoff energy were verified to be sufficient to obtain numerical convergence with acceptable computational costs. The optimization of BX was calculated in a $40 \times 15 \times 15 \text{ \AA}$ cubic cell with the gamma point as the Monkhorst-Pack k-point. The formal charge of BX ion was $-1 e$. All the atoms were allowed to relax during the calculation.

A perfect Sb_2S_3 (010) surface model used for the adsorption simulation is shown in Fig. 2, since the (101) plane is one of the most stable plane (Zakaznova-Herzog et al., 2006). The model consists of three layers of $(\text{Sb}_4\text{S}_6)_n$ ribbons with a 45-Å vacuum layer. The adsorption energy (ΔE_{ad}) of BX at the perfect $\text{Sb}_2\text{S}_3(010)$ surface was calculated according to the following equation:

$$\Delta E_{\text{ad}} = E_{\text{adsorbate+slab}} - E_{\text{adsorbate}} - E_{\text{slab}} \quad (1)$$

where $E_{\text{adsorbate+slab}}$ and E_{slab} are the total energies of the stibnite surface model after and before the adsorption of an adsorbate. Depending on the simulation cases, E_{slab} presents the energy of Sb_2S_3 (010) surface with or without an adsorbate; $E_{\text{adsorbate}}$ is the energy of Pb^{2+} or BX.

Additionally, the substitution energy of Pb^{2+} for Sb^{3+} at the stibnite surface is defined as:

$$E_{\text{sub}} = E_{\text{Pb}^{2+}}^{\text{total}} + E_{\text{Sb}^{3+}} - E_{\text{perfect}}^{\text{total}} - E_{\text{Pb}^{2+}} \quad (2)$$

where $E_{\text{Pb}^{2+}}^{\text{total}}$ and $E_{\text{perfect}}^{\text{total}}$ are total energies of bulk Sb_2S_3 with and without a Pb^{2+} ion. $E_{\text{Sb}^{3+}}$ and $E_{\text{Pb}^{2+}}$ are the energies of Sb^{3+} and Pb^{2+} , respectively.

To better discuss the geometry optimization results, partial atoms in the $\text{Sb}_2\text{S}_3(010)$ surface model were numbered, as shown in Fig. 3. The possible adsorption sites of Pb^{2+} at the surface were also noted in Fig. 3 and include the following: the sixfold hollow (6FH) site, the threefold

Download English Version:

<https://daneshyari.com/en/article/6672535>

Download Persian Version:

<https://daneshyari.com/article/6672535>

[Daneshyari.com](https://daneshyari.com)